



## RESEARCH ARTICLE

**EFFECT OF COPPER OXIDE ADDITION ON THE CHEMICAL PROPERTIES OF BARIUM STRONTIUM COBALT FERRITE- SAMARIUM DOPED CERIA CARBONATE CATHODE FOR SOLID OXIDE FUEL CELL APPLICATION****Muhammad Zul Idzham Abdul Ghani, Hamimah Abd.Rahman\*, Nurul Farhana Abdul Rahman, Umira Asyikin Yusop, Mohammad Fikrey Roslan, Sufizar Ahmad, Zolhafizi Jaidi***Faculty of Mechanical and Manufacturing Engineering, Universiti Tun Hussein Onn Malaysia, 86400 Parit Raja, Batu Pahat, Johor, Malaysia.*

**Abstract.** As a mixed oxygen ionic electronic conductor with high conductivity and exceptional catalytic activity for oxygen reduction and mobility, barium strontium cobalt ferrite (BSCF) is an excellent cathode for solid oxide fuel cells operating at intermediate temperatures. This composite cathode's ionic conductivity can be enhanced by increasing the electrode activity in oxygen reduction reactions, by adding certain catalyst materials. This study aims to determine how copper oxide (CuO) affects the BSCF-SDCC composite cathode. Wet ball milling was used to mix the powders, and were then calcined at 750 °C. The calcined BSCF-SDCC composite cathode powder was dry milled with the CuO at different weight percentages (1–5% wt%). After that, the powders were analyzed using a range of analytical methods. X-ray diffraction (XRD) was used to identify the phase and structure. Scanning electron microscopy (SEM) and energy dispersive spectroscopy (EDS) were utilized for microstructure observation and element analysis., Fourier transform infrared spectroscopy (FTIR) was used to analyze chemical bonds. The XRD measurements revealed the presence of secondary phases of  $2\theta$  at  $29^\circ$  and  $46^\circ$  in the BSCF-SDCC-CuO composite cathode powder. This condition can occur when the composite powder is blended using the ball milling method and is caused by an alkaline oxide reaction during the calcination process. FTIR studies showed a BSCF-SDCC-CuO bonding at  $1421\text{ cm}^{-1}$  and  $1423\text{ cm}^{-1}$ , respectively, whereas an asymmetric stretching vibrations band is suggested at  $1424\text{ cm}^{-1}$ . FTIR results show the connection between the metal oxides and the composites. In addition, SEM analysis displays that as the composition of CuO increases, the percentage of porosity decreases. These findings displayed that the CuO addition improved the chemical properties of the BSCF-SDC composite cathode powders.

**Keywords:** BSCF, cathode, copper oxide, SDCC, SOFC**Article Info**

Received 29 August 2024

Accepted 23 November 2024

Published 6 December 2024

**\*Corresponding author: hamimah@uthm.edu.my**

Copyright Malaysian Journal of Microscopy (2024). All rights reserved.

ISSN: 1823-7010, eISSN: 2600-7444

## 1. INTRODUCTION

A fuel cell is an electrochemical device that transforms the chemical energy into electrical energy and heat. Furthermore, compared to combustion-based heat engines, which involve a multi-step process involving a conversion from chemical energy to thermal energy to mechanical energy, fuel cells simply include a single step, which is from chemical energy to electrical energy [1]. For example, energy-generating combustion technologies will have an adverse impact on environmental issues. However, there were other benefits to fuel cells, including their distributed nature, low noise, excellent electrical efficiency, and fuel adaptability [2]. Among all fuel cell varieties, the Solid Oxide Fuel Cell (SOFC) has proven to be an extraordinary and promising power production technology since it can directly convert the chemical energy in fuels into electric power with high efficiency and low emissions. It could run on a range of fuels, produce no noise pollution, and employ clean methods to transform chemical energy into electricity [3]. Previous studies have shown that the production of the SOFC system required solid components and a crucial procedure that was costly and challenging to commercialize [4]. Because of this, conducting SOFC at intermediate temperatures (600–800 °C) is essential because it enables the use of reasonably priced metal alloys, which will reduce interfacial diffusion and electrode sintering [5].

Perovskite structure material has been shown in earlier studies to be a good and effective cathode material for solar organic fuel cells. This condition is reconsidered met by most perovskites, which include lanthanum, manganite, ferrites, and cobaltite [6]. The latest development in perovskites-structure materials, barium strontium cobalt ferrite (BSCF), has outstanding characteristics such as high conductivity, excellent catalytic activity for oxygen reduction and mobility, ionic conductivity, superconductivity, ferroelectricity, and magnetic resistance. [7]. Furthermore, the suitability of BSCF as a material for the solid cathode has been established. To improve cell performance and other qualities, it is important to mix various elements while forming a unique chemical [8]. The ionic conducting phase samarium doped ceria (SDC) was impregnated into a mixed conducting phase (BSCF) to considerably improve the electrochemical properties of a variety of innovative cathodes [9]. The SDC content has a major impact on the combination electrode's electrochemistry property. Samarium Doped Ceria offers reduced total costs, a longer stack lifetime, less interfacial losses with the cathode and anode, and increased oxygen ion conductivity [10].

The SOFC system's performance can be enhanced by the catalyst material. This material can speed up the anode and cathode processes. The addition of copper oxide (CuO), a superb catalyst material for oxygen surface adsorption, dissociation of molecular oxygen into atomic oxygen, and oxygen surface diffusion, improves the overall oxygen surface exchange kinetics of BSCF electrodes [11]. Previous study has shown that improving chemical reaction can be achieved by employing BSCF-SDCC composite cathode with addition of suitable catalyst [12]. The need for cathode and electrolyte materials can be improved with good intermediate-temperature fuel cell application. Therefore, the aim of this research was to determine the effects of CuO addition on the chemical properties of the BSCF-SDCC composite cathode powder.

## 2. MATERIALS AND METHODS

The mixture of 80 weight percent SDC powder and 20 weight percent binary carbonates used to make the composite electrolyte SDC carbonate (SDCC). The ratio of binary carbonates' molar proportions was 67:33 for  $Li_2CO_3$  and  $Na_2CO_3$  respectively. After that, all the powders, ethanol, and milling balls was combined, and dry ball milled for 24 hours at 150 rpm. Using a wet milling process, commercial BSCF and SDC powder was ground into BSCF-SDC composite cathode powder. The ratio of BSCF to SDCC is 50:50 in the composite powder. The two-hour milling process involved the utilization of high energy ball milling, with ethanol as the mixing medium. After mixing process, the powder was heated up at 90 °C for 12 hours to dry it out. The composite cathode powders crushed using an agate mortar after drying process. Then, copper oxide (CuO) was added to the BSCF-SDCC composite cathode powder in a weight range of 1% to 5% to carry out the dried-milling process. This

process of dry milling at 150 rpm was finished in 120 minutes. The sample was heated to 750 °C in an electric furnace for the calcination process following the milling procedure. Table 1 presents a summary of the sample identity.

**Table 1:** Identification of Sample

Sample	Amount of Copper Oxide (% weight)
BS-CuO0	0
BS-CuO1	1
BS-CuO2	2
BS-CuO3	3
BS-CuO4	4
BS-CuO5	5

To get the desired results about the chemical properties of BSCF-SDC when CuO was added, a few tests were required. X-ray diffraction (X-ray; Bruker D8 Advance, Germany) is one of the tests used to examine the sample's phase and crystalline structure. Unknown minerals, inorganic compounds, and crystalline materials are commonly identified using XRD. This research was performed using Cu K radiation at room temperature, with a wavelength of 0.15418. The step scanning of 0.02° with scanned diffraction pattern ranges from 20° to 90° was applied. The Eva Diffract Plus Software indicated to analyze the data. The equipment utilized for element characterization was a scanning electron microscope (SEM) (Hitachi Tabletop 3030, Japan) and energy dispersive spectroscopy (EDS). EDS uses a concentrated electron beam to emit the x-ray spectrum for a localized chemical analysis. For SEM and EDS investigation, gold coating was applied to the powder samples. Utilizing (Elmer Spectrum 100, USA), Fourier transform infrared spectroscopy (FTIR) was employed to assess the chemical bonding in the BSCF-SDCC-CuO composite cathode powder. This technique, based on scattering-type scanning near field optical microscopy, creates infrared images with nanoscale spatial resolution by capturing the infrared light dispersed at a scanning probe tip. Some composite powder was applied to the sample container to perform the test using the attenuated total reflection (ATR) method. The software Spectra Express (version 1.3.2) was utilized to analyze the infrared spectra, which were captured within the wave range of 550 to 4000 cm<sup>-1</sup>.

### 3. RESULTS AND DISCUSSION

#### 3.1 Phase Analysis by XRD

XRD analysis was performed on BS-CuO0 and BS-CuO5 composite cathode powder, and the findings are displayed in Figure 1. The material has a phase structure with JCPDS no. 00-005-0563 (cubic crystal) for BSCF, JCPDS no. 01-075-0157 (faced-center cubic) for SDCC, and JCPDS no. 03-004-0743 (faced-center cubic) for CuO, according to the data gathered. The basic material's intensity pattern is produced at a common spectrum. To obtain the final product, the BSCF-SDCC-CuO composite cathode powder must go through several phases of production. The major component of the sample, which is iron carbonate (FeCO<sub>3</sub>), and barium carbonate (BaCO<sub>3</sub>) did not appear to change in phase or crystallinity even after all phases had occurred. On the other hand, secondary phases of the iron carbonate (FeCO<sub>3</sub>) and barium carbonate (BaCO<sub>3</sub>), with JCPDS numbers 01-083-1764 and 01-071-2394 respectively, are visible in the XRD diffraction peaks. It is anticipated from Figure 1 that the secondary peaks will appear when they approach the BSCF and SDC peaks. This results from the reaction between alkaline oxide and CO<sub>2</sub> during the calcination process. Previous studies have shown that following the calcination process, there were still several ways for this secondary phase or impurity ions to be present in the BSCF system [13]. The HEBM process, which requires mixing at a high speed that causes the particle to shatter due to impact forces generated during the conversion of kinetic energy, may also have contributed to the formation of impurities in the composite powder [14]. The intense peak location of iron carbonate (FeCO<sub>3</sub>), and barium carbonate (BaCO<sub>3</sub>) is in line with the observations made in previous studies, which is 2 θ at 29° and 46°. However, the presence of impurities in the BSCF

material has caused the crystallite percentage to alter to 25.73%, even though SDC is still stable in the original crystallite phase [15]. The crystallite percentage was calculated using OVA software.

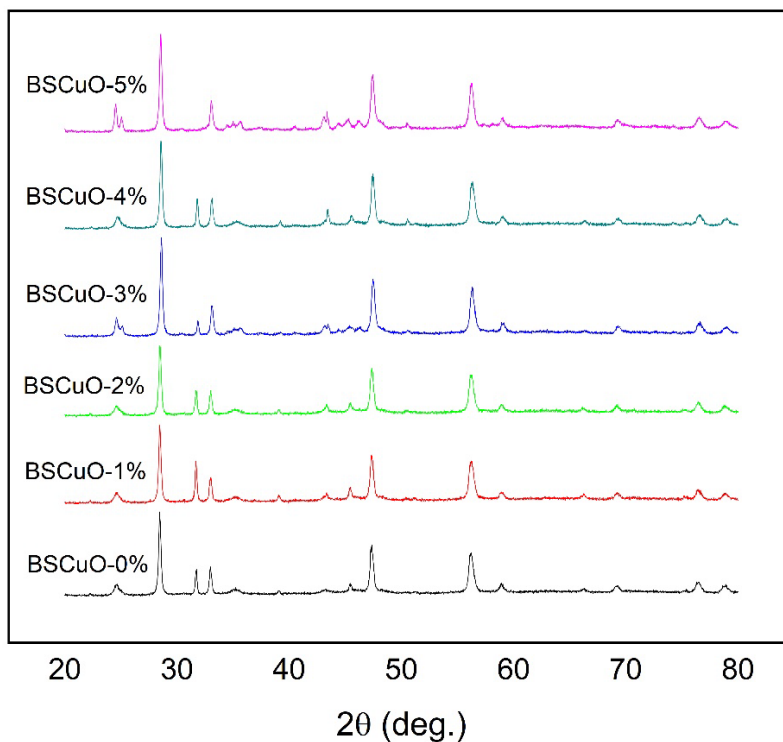


**Figure 1:** XRD profiles of BS-CuO-0%, BS-CuO-1%, BS-CuO-2%, BS-CuO-3%, BS-CuO-4% and BS-CuO-5%.

### 3.2 Elemental Analysis by EDS and Morphologies Analysis by SEM

The elements present in the EDS spectra of Figure 2a and 2b are those of the commercial samples BSCF, SDCC, and CuO that were utilized in this experiment. Numerous elements, including Barium (Ba), Strontium (Sr), Cobalt (Co), Ferum (Fe), Samarium (Sm), Ceria (Ce), Natrium (Na), and Copper (Cu), were included in the composition of the cathode powder composite. All these essential elements were documented by the BS-CuO0 until BS-CuO5 samples. During the milling procedure, they were mixed uniformly and dispersed equally. Aside from that, each element's EDS weight and mole percentage values are presented. The particle shape from the SEM observation is shown in Figure 3. The values obtained from the SEM results were examined using Image J. The top surface section image may be used to determine porosity to increase accuracy and precision. Furthermore, the process of calcination can remove any leftover carbon dioxide from the powder, allowing carbonate to transform into the necessary BSCF phase with a transparent crystal perovskite structure [16]. The link created by the calcination process, which reinforced the links between each element, lead to agglomeration [17]. Consequently, the porosity will be more precise and consistent with the overall porosity of the samples with this SEM analysis.

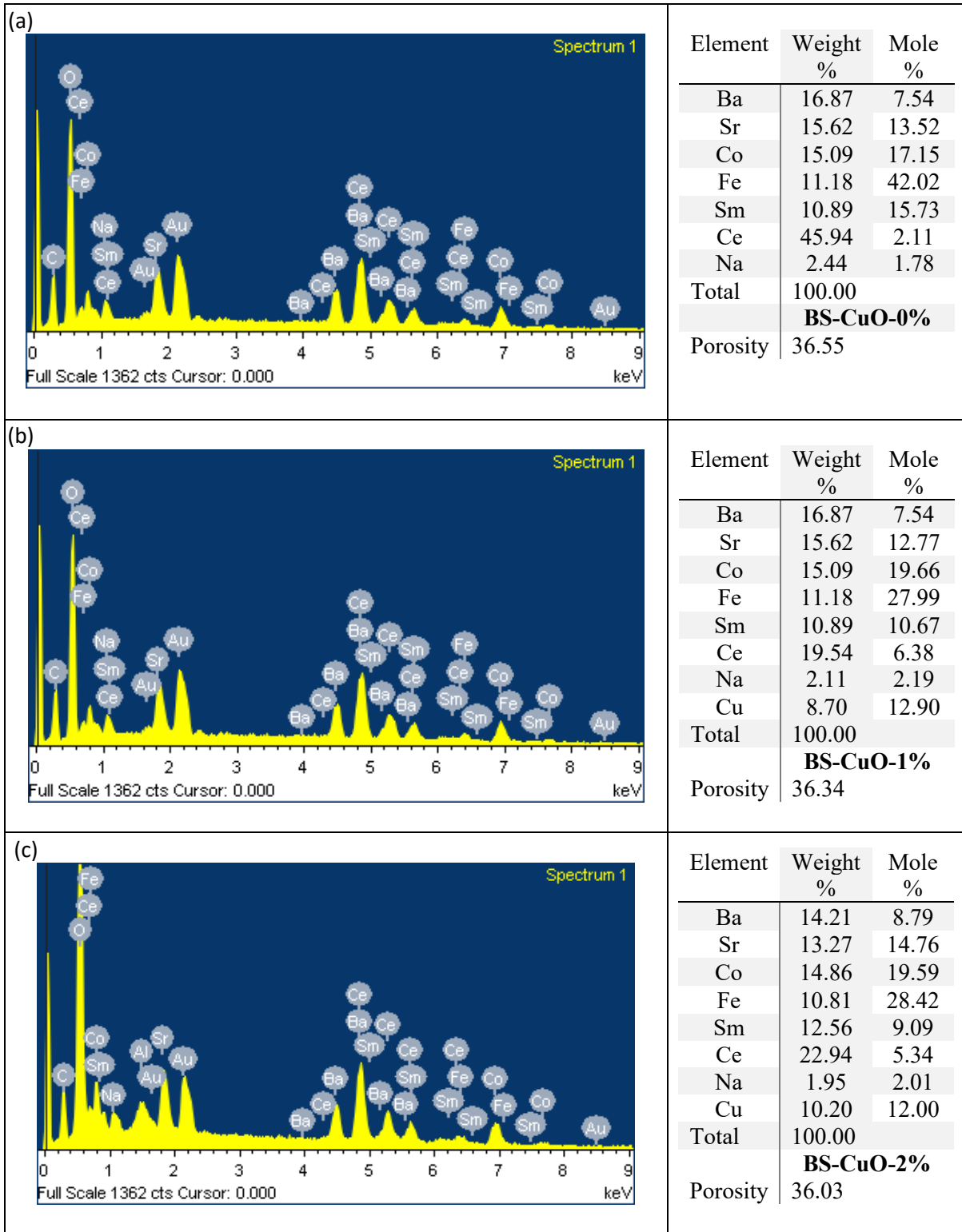


**Figure 2a:** EDS Spectrum of (a) BS-CuO-0%, (b) BS-CuO-1% and (c) BS-CuO-2%

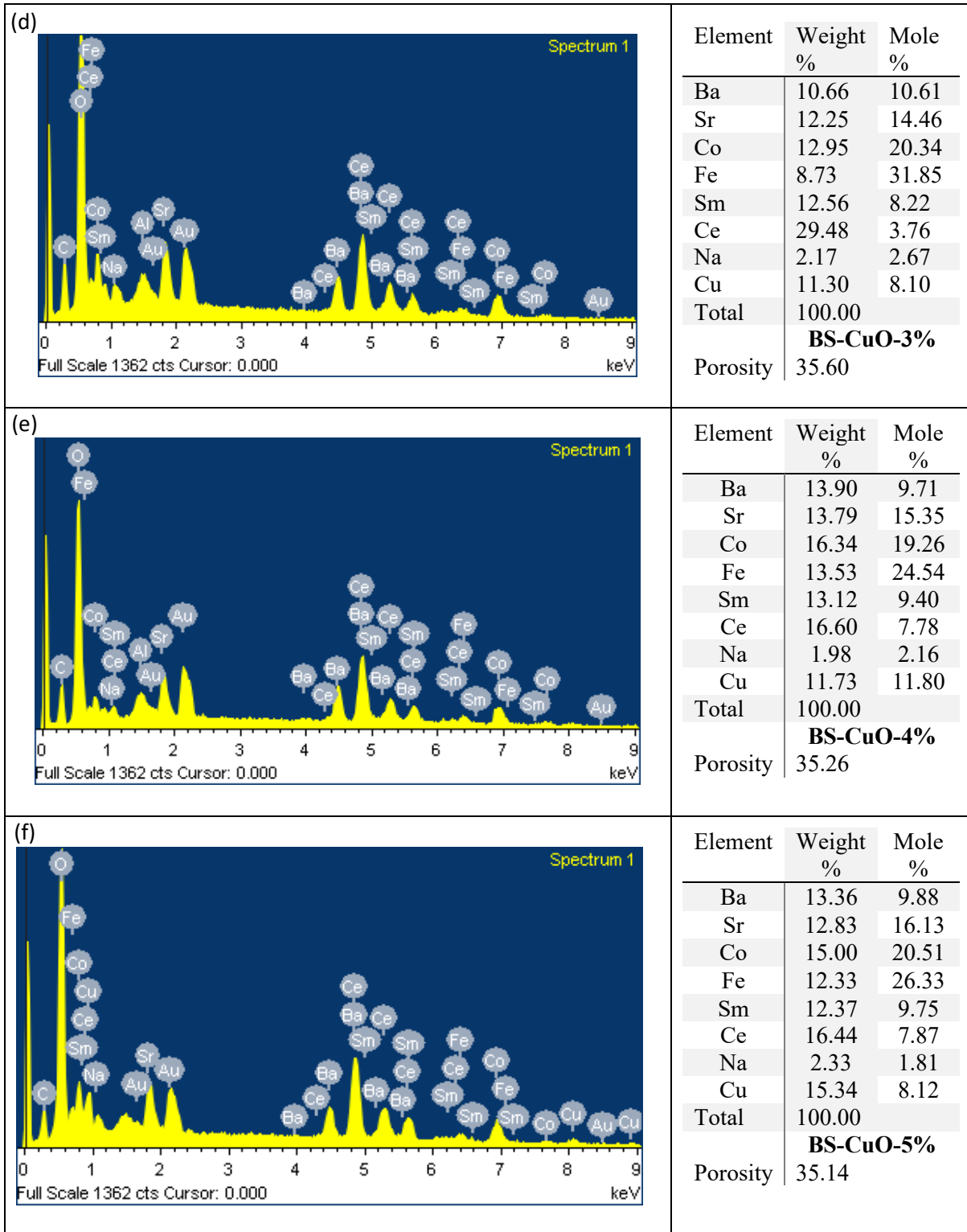


**Figure 2b:** EDS Spectrum of (d) BS-CuO-3%, (e) BS-CuO-4% and (f) BS-CuO-5%.

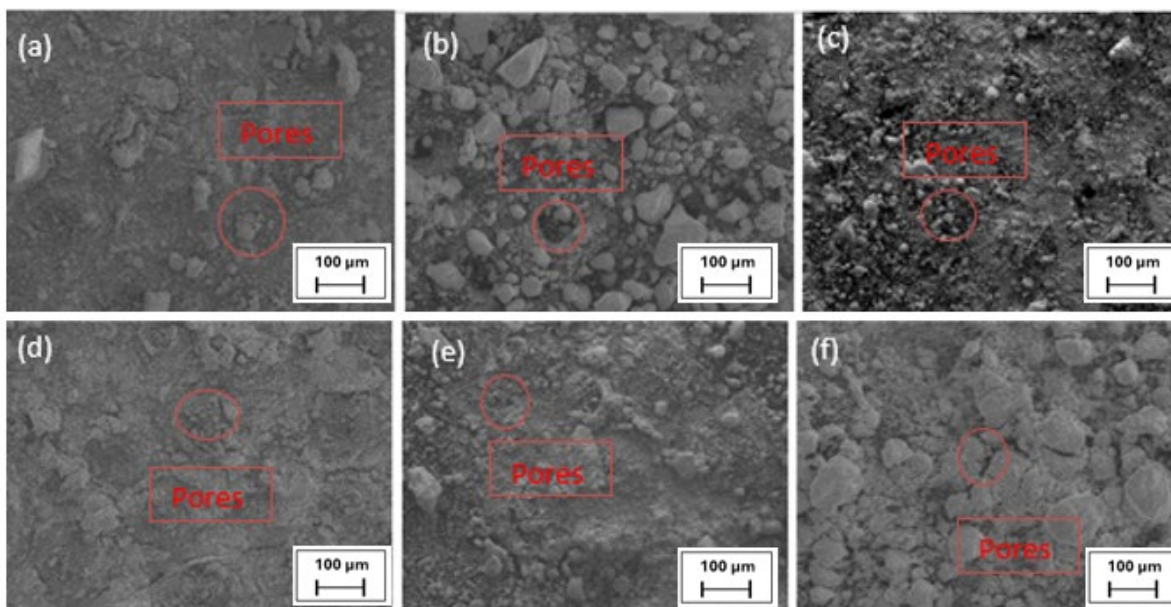


**Figure 3:** SEM morphology of; (a) BS-CuO0, (b) BS-CuO1, (c) BS-CuO2; (d) BS-CuO3, (e) BS-CuO4 and (f) BS-CuO5.

### 3.3 Chemical Bonding Analysis by FTIR

FTIR was used to analyze the chemical bonding in the BS-CuO0 and BS-CuO5 composite cathode powders, with the results displayed in Figure 4. The investigated spectra had a wavenumber range of  $4000\text{--}550\text{ cm}^{-1}$ . For determining infrared transmittance and other related properties, such as the functional group of organic compounds, FTIR was a very useful technique [18]. The FTIR data for each of the produced composite cathode powders are summarized in Table 2. Every composition shows a composite of six different compositions. Analyzing infrared ray transmittance lines is essential for identifying the functional group of organic compounds. A band of hydrogen (O-H) bond developed at wavenumbers  $3000\text{ to }4000\text{ cm}^{-1}$  because of water adsorption caused by interactions between the sample and its environment, as seen in Figure 4 [19]. Carbon bonding occurs at  $1421\text{ and }853\text{ cm}^{-1}$ , respectively, and two prominent peaks that correspond to the molecules BS-CuO1% and BS-CuO5% are seen on this graph. The same carbon bonding was shown to develop at  $1423\text{ and }859\text{ cm}^{-1}$  for BS-CuO2%, BS-CuO3%, and BS-CuO4% from the Figure 4. A bonding band exists between  $1421\text{ and }1423\text{ cm}^{-1}$  and is frequently brought on by  $\text{CH}_2$  bending vibration. Furthermore, the absorption bands that occurred between  $800\text{ and }4200\text{ cm}^{-1}$  are commonly caused by the development spectra of the final calcined powder as well as the synthesis of metal oxide linkages such as Ba-O, Sr-O, Co-O, and Fe-O. As the amount of CuO added to BSCF-SDCC increased, the porosity of the BSCF-SDCC-CuO electrolyte decreased and lowered the cathode's sintering temperature.

**Table 2:** FTIR results of BS-CuO-0% and BS-CuO (1-5wt %) composite cathode powder.

Composite	Wave number ( $\text{cm}^{-1}$ )	Functional group
All	3000-4000	Hydrogen (O-H) bond
BS-CuO-0%	1383-1434	Carbonate ( $\text{CH}_3$ ) bending
	853-859	Carbonate ( $\text{CH}_2$ ) out-of-plane bending
BS-CuO (1-5wt %)	1421-1423	Carbonate ( $\text{CH}_2$ ) bending
	586-857	Metal oxides bonds

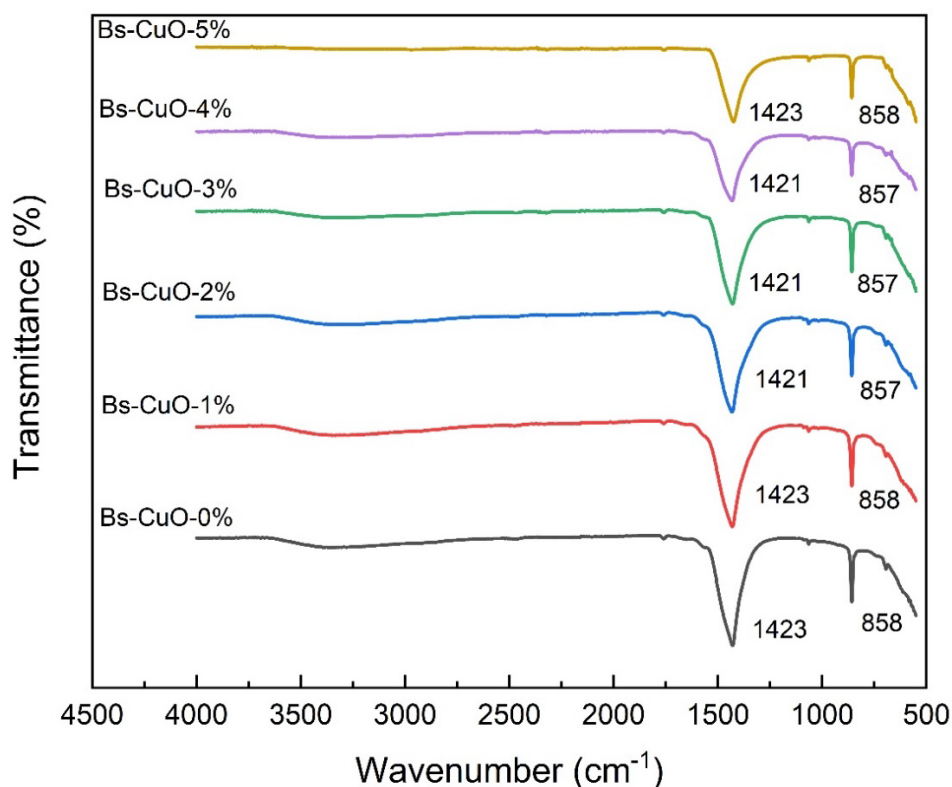


**Figure 4:** FTIR spectrum graph for BS-CuO-0%, BS-CuO-1%, BS-CuO-2%, BS-CuO-3%, BS-CuO-4% and BS-CuO-5%.

#### 4. CONCLUSIONS

This work proposes to investigate and assess the effects of CuO addition on the chemical properties of BSCF-SDCC composite cathode powder. To sum up, all the tests that were taken showed a positive correlation. The XRD results show that secondary peaks ( $\text{BaCO}_3$  and  $\text{FeCO}_3$ ) were formed during the composite powder's calcination process. The secondary peaks may arise because of the alkaline earth oxide elements (Ba and Sr) reacting with  $\text{CO}_2$  during the heat treatment procedure. The SEM morphology data show that there is an increase in particle shape and a tendency for the sample to agglomerate with an increase in CuO addition. Furthermore, the EDS spectrum graph showed the quantitative amount that each atom of the composite cathode material contained in addition to the peak of each element. The calcined BSCF-SDCC composite powders' growth spectra are examined, along with the creation of metal oxide connections including Ba-O, Sr-O, Co-O, and Fe-O. The addition of copper as a unique bonding element is supported by the existence of CuO, as determined by EDX analysis, which adds to the overall stability of the composite. Additionally, as demonstrated by SEM micrographs and Image J analysis, increasing CuO content causes a decrease in porosity, suggesting improved structural integrity. Surprisingly, great care must be taken while selecting a material and parameter to avoid unexpected impacts on the properties and stability of the composite cathode powder. It is believed that the BSCF-SDCC composite cathode powder's characteristics will improve with the addition of CuO. As a result, further research is required on the conductivity of the BSCF-SDCC-CuO composite cathode.

## Acknowledgements

This research was supported by the Universiti Tun Hussein Onn Malaysia (UTHM) through Tier 1 (Vot Q494).

## Author Contributions

All authors contributed toward data analysis, drafting and critically revising the paper and agree to be accountable for all aspects of the work.

## Disclosure of Conflict of Interest

The authors have no disclosures to declare.

## Compliance with Ethical Standards

The work is compliant with ethical standards.

## References

- [1] Singh, M., Zappa, D. & Comini, E. (2021). Solid oxide fuel cell: Decade of progress, future perspectives and challenges. *International Journal of Hydrogen Energy*, 46(54), 27643–27674.
- [2] Van Biert, L., Visser, K. & Aravind, P. V. (2020). A comparison of steam reforming concepts in solid oxide fuel cell systems. *Journal of Application Energy*, 264(11), 114748.
- [3] Afroze, S., Karim, A. H., Cheok, Q., Eriksson, S. & Azad, A. K. (2019). A Review: Latest development of double perovskite electrode materials for solid oxide fuel cells. *Journal Frontiers of Energy*, 13(4), 770–797.
- [4] Dwivedi, S. (2020). Solid oxide fuel cell: Materials for anode, cathode and electrolyte. *International Journal of Hydrogen Energy*, 45(44), 23988–24013.
- [5] Lyu, Y., Xie, J., Wang, D. & Wang, J. (2020). Review of cell performance in solid oxide fuel cells. *Journal of Material Science*, 55(17), 7184–7207.
- [6] Xia, W., Li, Q., Sun, L., Huo, L. & Zhao, H. (2020). Enhanced electrochemical performance and CO<sub>2</sub> tolerance of Ba<sub>0.95</sub>La<sub>0.05</sub>Fe<sub>0.85</sub>Cu<sub>0.15</sub>O<sub>3-δ</sub> as Fe-based cathode electrocatalyst for solid oxide fuel cells. *Journal Europe Ceramic Society*, 40(5), 1967–1974.
- [7] Zhao, S., Tian, N. & Yu, J. (2020). Performance of Ba<sub>0.5</sub>Sr<sub>0.5</sub>Co<sub>0.8</sub>Fe<sub>0.2</sub>O<sub>3-δ</sub>/Ce<sub>0.85</sub>Sm<sub>0.15</sub>O<sub>2-δ</sub>-CuO as a cathode for intermediate temperature solid oxide fuel cells. *Journal of Alloys and Compound*, 825, 154013.
- [8] Plazaola, A. A. (2019). Mixed ionic-electronic conducting membranes (MIEC) for their application in membrane reactors: A Review. *Journal of Processes*, 7(3), 128.
- [9] Yusop, U. A., Rahman, H. A. & Tan, K. H. (2019). Effect of Ag addition on the structural properties of Ba<sub>0.5</sub>Sr<sub>0.5</sub>Co<sub>0.8</sub>Fe<sub>0.2</sub>O<sub>3-δ</sub>-Sm<sub>0.2</sub>Ce<sub>0.8</sub>O<sub>1.9</sub> composite cathode powder. *International Journal of Integrated Engineering*, 11(7), 169–174.

- [10] Rahman, N. F. A., Ismail, A., Azmi, M. A., Mahzan, S. & Rahman, H. A. (2022). Phase stability of LSCF/YSZ-SDC & LSCF/YSZ-SDCC dual composite cathode solid oxide fuel cell. *Research Progress in Mechanical and Manufacturing Engineering*, 3(1), 1065-1074.
- [11] Jaidi, Z., Azmi, M. A., Abd Rahman, H., Huai, T. K., Yusop, U. A., Ghani, M. Z. I. A. & Roslan, M. F. (2023). The effect of milling duration to the structural properties of silica from rice husk. *Malaysian Journal of Microscopy*, 19(1), 193-201.
- [12] Yusop, U. A., Huai, T. K., Rahman, H. A., Baharuddin, N. A. & Raharjo, J. (2020). Electrochemical performance of barium strontium cobalt ferrite-samarium doped ceria-silver for low temperature solid oxide fuel cell. *Material Science Forum*, 991(1), 94-100.
- [13] Tian, N., Qu, Y., Men, H., Yu, J., Wang, X. & Zheng, J. (2020). Properties of  $\text{Ce}_{0.85}\text{Sm}_{0.15}\text{O}_{2-\delta}$ -CuO electrolytes for intermediate-temperature solid oxide fuel cells. *Journal of Solid State Ionics*, 351, 115331.
- [14] Yang, P. Li. Q., Zhang, H., Yao, M., Yan, F. & Fu, D. (2020). Effect of Fe, Ni and Zn dopants in  $\text{La}_{0.9}\text{Sr}_{0.1}\text{CoO}_3$  on the electrochemical performance of single-component solid oxide fuel cell. *International Journal of Hydrogen Energy*. 45(20), 11802-11813.
- [15] Zolhafizi, J., Azmi, M. A., Rahman, H. A., Zakaria, H., Hassan, S., Mahzan, S., Ismail, A., Ariffin, A. M. T., Tukimon, M. F., Yusof, U. A. & Baharuddin, N. A. (2023). Samarium doped ceria (SDC) electrolyte modification by sintering aids addition to reducing sintering temperature: A Review. *Jurnal Kejuruteraan*, 35(1),65-76.
- [16] Yousaf, M., Mushtaq, N., Zhu, B., Wang, B., Akhtar, M. N., Noor, A. & Afzal, M. (2020). Electrochemical properties of  $\text{Ni}_{0.4}\text{Zn}_{0.6}\text{Fe}_2\text{O}_4$  and the heterostructure composites (Ni-Zn ferrite-SDC) for low temperature solid oxide fuel cell (LT-SOFC). *Electrochimica Acta*, 331, 135349.
- [17] Kuntiyi, O., Shepida, M., Sozanskyi, M., Yuriy Sukhatskiy, Y., Mazur, A., Kytsya, A. & Bazylyak, L. (2021). Sonochemical Synthesis of silver nanoparticles in sodium polyacrylate solution. *Biointerface Research in Applied Chemistry*, 11(4), 12202-12214.
- [18] Wang, Z., Lv, P., Yang, L., Guan, R., Jiang, J., Jin, F. & He, T. (2020).  $\text{Ba}_{0.95}\text{La}_{0.05}\text{Fe}_{0.8}\text{Zn}_{0.2}\text{O}_{3-\delta}$  cobalt-free perovskite as a triple-conducting cathode for proton-conducting solid oxide fuel cells. *Ceramics International*. 46(11), 18216-18223.
- [19] Kim, S. Y. & Li, J. (2021). Porous mixed ionic electronic conductor interlayers for solid-state batteries. *Energy Materials Advances*, 2021, 1519569.